Positional accuracy evaluation of declassified Hexagon KH-9 mapping camera imagery

Arzhan Surazakov and Vladimir Aizen

Abstract

This paper examines the positional accuracy of the declassified KH-9 Hexagon imagery and derived DEM. Aimed at geodesy and mapmaking, the KH-9 program (1973-1980) resulted in an image archive with worldwide stereo coverage at 6-9 m. We used six KH-9 images acquired in 1980 over two testfields in Central Asia. Using reseau marks on the scanned KH-9 frames, we found and corrected image distortions. In bundle orientation with Ground Control Points (GCPs) from Quickbird images, we achieved horizontal accuracies below 6 m for a flat terrain testfield and approximately 10 m for a mountainous terrain testfield. With three GCPs the image orientation horizontal accuracy degraded by only 20%. We generated a DEM from the KH-9 images and estimated its vertical accuracy using IceSAT laser altimetry data and an additional DEM from 1:25,000 topographic maps. The DEM RMSE was 6.18 m over flat terrain and 20.0 m over mountainous terrain.

Introduction

Although archival satellite imagery is of great value for Land Cover/Land Use Change (LCLUC) studies, the archive of KH-9 of high resolution space photographs (29,000 images) declassified in 2002 remains, to our knowledge, largely untapped. Aimed at reconnaissance and mapmaking, the KH-9 program (codename Hexagon) was developed by the US military as a successor to KH-4 Corona program (Richelson, 2001). The Hexagon mapping program, operated from 1973 to 1980, accomplished its goal of near worldwide stereo coverage at 6-9 m. Until this study, however, the imagery has not been rigorously evaluated and/or used in LCLUC studies.

The potential of the KH-9 archive for LCLUC studies lies in the vast information it contains, and the state-of-the-art metric quality of the photographs. The KH-9 frame camera, with precision reseau grid, allows accurate reconstruction of the image geometry, and photogrammetric processing in off-the-shelf software.

A. Surazakov (arzhan@uidaho.edu) and V. Aizen are with the Department of Geography, the University of Idaho, McClure Hall 203, Moscow, ID 83844-3021

Acquired with 70% endlap, these photographs enable Digital Elevation Model (DEM) generation, and strongly reduce the number of needed Ground Control Points (GCPs). A KH-9 photograph has nearly the same ground footprint as a Landsat MSS image (the two programs started approximately at the same time), but 177 times the resolution. The KH-9 scanned data is now available to the public at a nominal price.

Unlike the complete declassification of Corona, Argon and Lanyard programs in 1995 (e.g., Day *et al.*, 1998; Galiatsatos, 2004; McDonald, 1995; Peebles, 1997), the KH-9 mission-related documentation remains classified. A one-page press release (National Archives and Records Administration, 2002) and a few details (NGA, 2002; Richelson, 2001; Peebles, 1997), most of which are only of historical value, constitute the current knowledge about the program and the data. To get an insight into the possible system characteristics of the KH-9 frame camera, and to select proper film scanning resolution, we suggest and provide evidence that the KH-9 frame camera and the well known NASA Large Format Camera (LFC) flown onboard Space Shuttle mission STS 41-G (1984) have similar design.

In this paper, we analyze two KH-9 image triplets acquired over two test sites in Central Asia; one of flat terrain and another of mountainous terrain. We estimate image distortions using reseau grids. For image orientation, we use GCPs from Quickbird imagery (Google Earth™ data); using IceSAT and map-based DEMs, we estimate the vertical accuracy of the KH-9 DEMs.

Background

KH-9 Hexagon mapping program

By the end of 1960s, Corona reached its technological limits, and a new system with higher spatial resolution and larger coverage was needed for US strategic reconnaissance (Richelson, 2001). Development of the new system, KH-9 Hexagon, was subcontracted to Itek, but later it was transferred to Perkin-Elmer. The main payload on the KH-9 platform was two cameras (60 inch focal length) that produced images with 0.9 m resolution (some sources cite 0.6 m). On twelve of the twenty KH-9 missions (numbers 1205 through 1216),

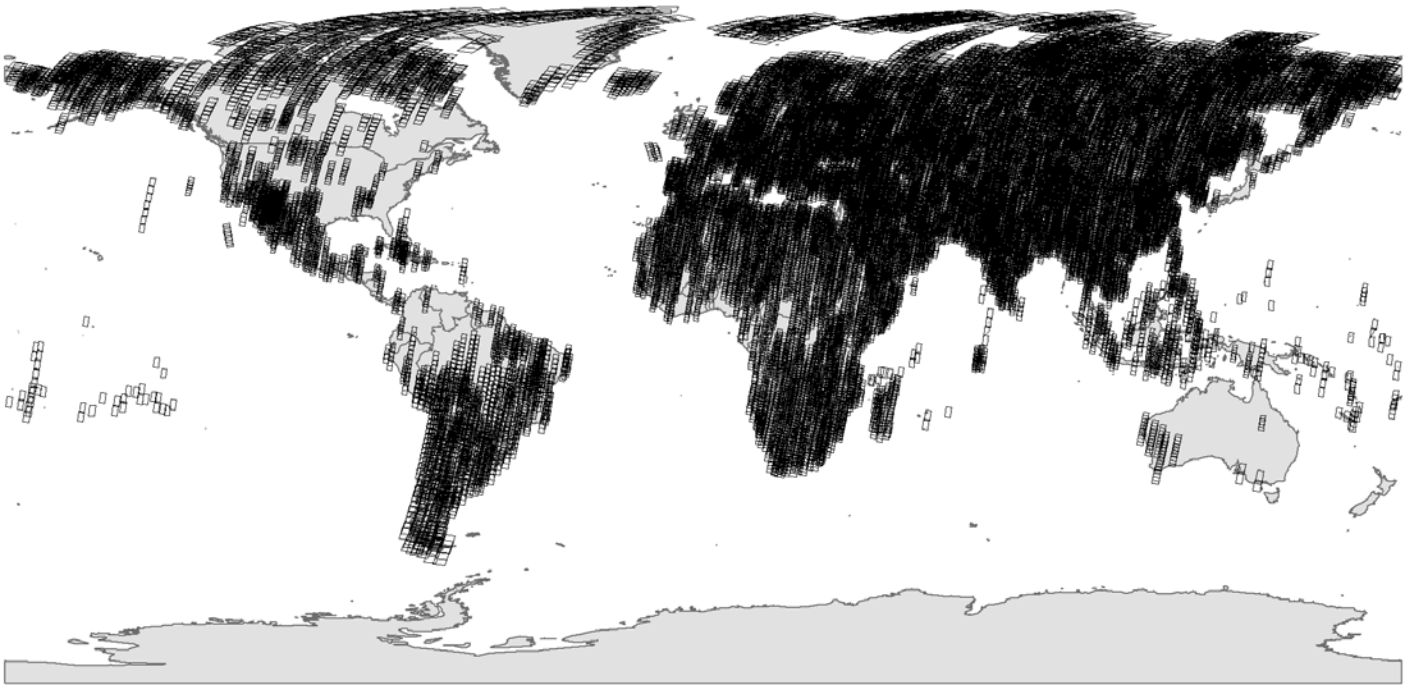

Figure 1. Coverage of the KH-9 mapping camera archive (data from U.S. Geological Survey (USGS).

the primary cameras were complemented with a frame mapping camera (twelve inch focal length) (Peebles, 1997). One may suggest that the KH-9 platform combined enhanced versions of both the Corona and Argon optical systems for mapmaking. Argon frame camera (three inch focal length, 124 m ground resolution) provided global geodetic framework, while panoramic Corona cameras produced high resolution imagery for large scale mapping (up to 1:50,000) (Baclawski, 1997; Day *et al*., 1998).

The KH-9 mapping camera acquired approximately 29,000 photographs worldwide, largely excluding inner Greenland, Antarctica and Australia (Figure 1). In 2002, the U.S. Government declassified all of the KH-9 mapping camera images, excluding approximately 100 images over Israel. Imagery from the two primary cameras remains classified; in this paper, we refer only to the mapping camera imagery.

KH-9 Mapping camera and Large Format Camera

Because the design of the KH-9 mapping camera remains classified, we investigated the NASA Large Format Camera (LFC) flown onboard Space Shuttle mission STS 41-G (1984) to develop an insight into possible KH-9 mapping camera design and performance. Both frame cameras were built for space-based topographic mapping, and were designed by the same private contractor, Itek. We hypothesize that when Itek built the LFC for NASA, they may have reused the already proven design of the KH-9 mapping camera. Here are the known similarities: Both cameras used 23x46 cm frame format with the long dimension along the flight direction, and used the same 30.5 cm focal length (Mollberg and Schardt, 1988). The LFC film capacity (2400 frames) multiplied by the number of KH-9 missions with the mapping camera (twelve) equals 28800 images, which is the approximate number of declassified KH-9 images. The identified differences of the cameras are in the number of reseau marks (1058 in KH-9 and 45 in LFC) and fiducials (four in KH-9 and 12 in LFC).

The LFC differs from standard aerial survey cameras in that it has greater film capacity and twice the image frame size, and provides its own pressure and thermally conditioned environment (Table 1). The camera underwent extensive preflight calibration and met all design specifications (Mollberg and Schardt, 1988).

The LFC photography was found to be suitable for topographic mapping up to 1:100,000 scale (Ali 1993; Togliati and Moriondo 1986; Newton and Derenyi 1986; Derenyi and Newton 1986). The positional accuracy of LFC data ranged from 7 to 27 m horizontally and from 7 to 30 m vertically. We may expect at least this level of performance from the KH-9 data because of the lower operational altitudes of KH-9 satellite (171 km vs. 225, 272 and 352 km for the LFC (Mollberg and Schardt 1988).

TABLE 1. CHARACTERISTICS OF THE LFC (MOLLBERG AND SCHARDT, 1988)

Lens:	
Focal length	30.5 cm
Resolution AWAR	88 line pairs/mm
Max distortion	<20µm
Automatic exposure control	1/250 to 1/30 sec
Interchangeable haze and minus blue filters	
Magazine:	
Format	23 by 46 cm
Forward overlap	10, 60, 70 or 80%
Film capacity	2400 frames
Adjustable forward motion compensation	

Data

Testfields

We selected two separate testfields, one of flat terrain and another of mountainous terrain, to estimate the variability of the accuracy of the KH-9 images under different terrain conditions. The first testfield lies in the Tarim river basin in NW China (120 x 120 km, centered at 39°18'N 76°15'E). Located at elevations of 1,100 – 1,600 m, the area is characterized by irrigated agricultural plots and barren dry land (Figure 2, black box on the left image). The second testfield surrounds the Akshiirak range in the Tien Shan mountains of Kyrgyzstan (55 x 45 km, centered at 41°51'N 78°18'E). Here the elevation ranges from 1,600 to 5,120 m, and above 3,500 m, the area is heavily glaciated (Figure 2, black box on the right image).

Image data

In this study we used six KH-9 photographs acquired during the last KH-9 mission (1216) in 1980 (Figure 2). The Tarim testfield was imaged on September 7th and the Akshiirak testfield was imaged on August 21st. The photographs were taken at a flying altitude of 171 km with 70% endlap so that each testfield appears on three consecutive photographs forming a stereo triplet. Each frame covers an area of about 250x125 km on the ground.

The data provider, the Center for Earth Resources Observation and Science (EROS) of the USGS, scanned the third generation film negatives at 14 µm. EROS also offers scanning at 7 µm and 21 µm, but from the suggested KH-9 and LFC similarity of camera design we determined that the 14 µm option balances both the goal of our work (positional accuracy assessment) and

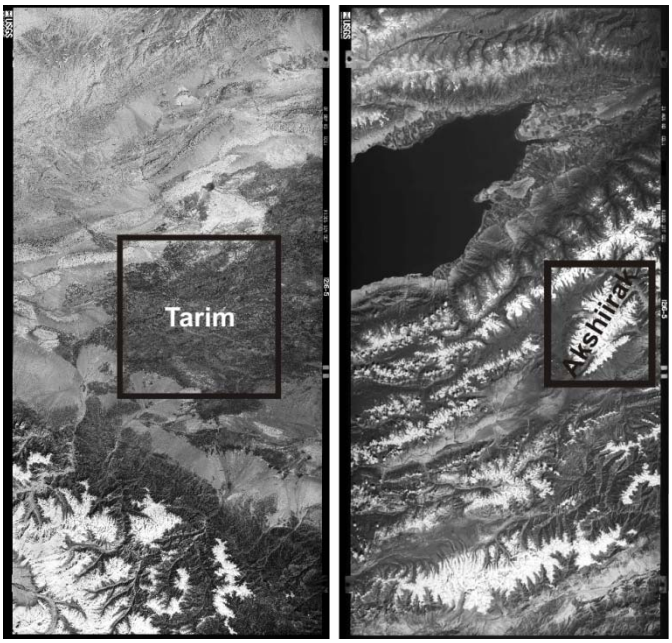

Figure 2. The center images of the KH-9 triplets over the flat (left) and mountainous (right) testfields. The testfields occupy only portions of the images as shown by black boxes.

data volume. It has been found in laboratory tests with low contrast targets (2:1), that the combination of LFC and Kodak 3414 High Definition film resulted in 80 lp/mm resolution (Mollberg and Schardt, 1988). To maximize fine detail, the LFC system resolution and the Kell factor suggest the 7 µm option. However, atmospheric haze, residual motion blur and the third generation of the KH-9 film stored at EROS would degrade the laboratory determined resolving power. Also, 2.6 Gb image file at 7 µm is difficult to handle, especially in a project using many KH-9 images. At 14 µm, the file size reduces to manageable 0.6 Gb with only a minor loss in the accuracy of image orientation and DEM generation (Baltsavias, 1999).

EROS scanned the KH-9 photographs using Leica DSW700 photogrammetric flat bed scanner. Shortly before the images were processed for this study, the manufacturer geometrically calibrated the scanner and confirmed its excellent accuracy (RMSE X 0.644 µm, Y 0.532 µm in b/w mode) (USGS 2008, personal communication). Due to the large frame size, the photographs were scanned as 8 bit TIFFs in two segments with about 1 cm overlap.

Image preprocessing

To achieve the highest positional accuracy with the very large format KH-9 data, we had to account for image distortion introduced by development and double duplication of the film and almost three decades of

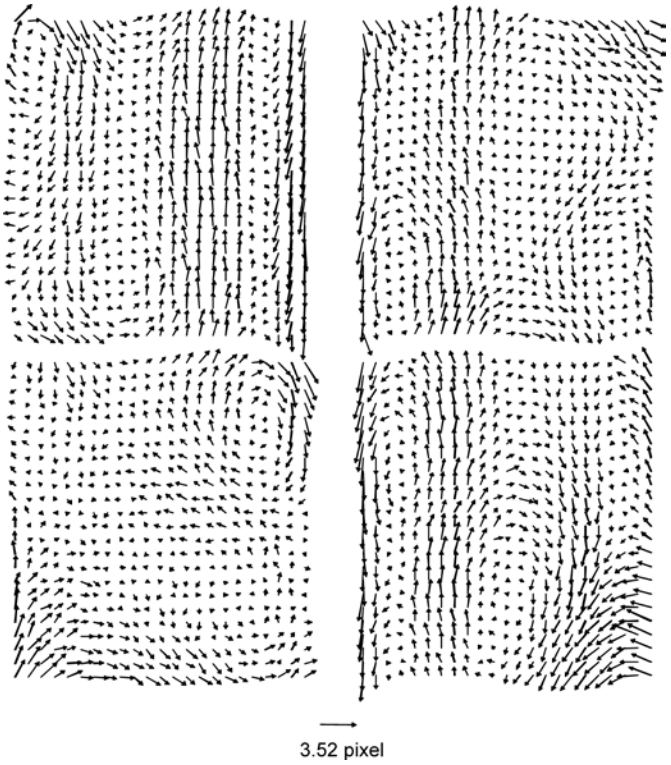

Figure 3. Distortion fields of the KH-9 images on Figure 2. For each image, the distortion fields are shown apart for separately scanned frame segments (upper and lower halves). The vectors show shift of the reseau crosses from image to nominal positions (14 μm pixel size).

storage. The precision reseau grid overlaid on the KH-9 photographs provided an opportunity to reconstruct the image geometry that existed at the moment of film exposure. To achieve this, in each digitized frame we located 1058 reseau crosses with subpixel precision. Image distortion fields were estimated using residuals from least square adjustment of image and nominal coordinates (assuming exactly 10 cm grid spacing) of the crosses (Figure 3).

The average image distortion of the six KH-9 images was 0.91 pixel (12.74 μm) reaching up to 4.92 pixel (68.88 μm) at the edges and corners of the frames. The distortion vectors that were larger than 0.5-0.6 pixel generally followed locally systematic but globally non-uniform pattern. The distortion patterns also were different among all six images thus emphasizing the need for individual image calibration. The complex distortions could not be removed by a global rectification algorithm such as affine transformation. We used Thin Plate Spline (TPS) local interpolation with bilinear resampling to generate the corrected images. The corrected images were limited to the reseau grid area leaving out the four fiducial marks. In place of

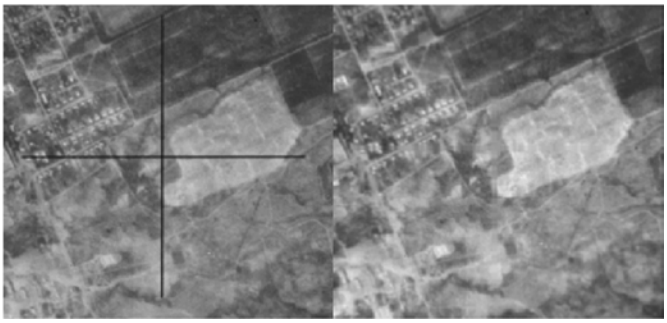

Figure 4. A fragment of the KH-9 original image (left) and after the reseau cross was located and filled with neighbor values (right).

fiducials we used the center of the reseau grid to approximate the image principal point.

Before applying the TPS rectification, we used the image reseau coordinates to fill the reseau footprints with neighbor pixel values (Figure 4). The reseau crosses are not part of the imaged terrain and may confuse Automatic Terrain Extraction (ATE) that searches for similar terrain features on conjugate images. In our tests with Leica Photogrammetry Suite 9.2 (LPS), ATE failed to run on a KH-9 stereopair with reseau crosses still present on the images. We automated all of the geometric calibration procedures in KH_TOOLS software implemented in Interactive Data Language 7.0.1 (IDL).

The quality of the scanned images was very good: nearly scratch and dirt free, very limited presence of Newton rings (mostly at the frame edges), no noticeable vignetting, and radiometric noise visible only on bright snow-covered glaciers. To enhance the local contrast for automatic image matching, we applied a Wallis filter. Brightness variations across an image were corrected with ImageEqualizer, a color balancing application included in LPS.

Bundle orientation

Image orientation and DEM generation were performed in Leica Photogrammetry Suite™ 9.2 (LPS). Since KH-9 images were acquired under perspective geometry, we used frame camera model. No additional parameters such as lens and film distortions were used in triangulation, except for a correction for earth curvature (an optional parameter in LPS). GCPs for both testfields were collected from orthorectified Quickbird imagery available in Google Earth™ (with permission from Google™). Vertical coordinates were collected from SRTM version 1 (unedited) DEM that produced better results than with Google Earth™ elevations.

TABLE 2. SENSITIVITY OF THE BUNDLE ORIENTATION TO DIFFERENT NUMBER OF GCPS

Control points	Check points	RMSE of check points		
		X, m	Y, m	Z, m
30	3	5.88	2.80	5.76
20	13	5.05	3.03	5.97
10	23	4.58	3.50	6.18
3	30	5.38	4.51	7.28

Tarim testfield

The Tarim KH-9 triplet was oriented using 33 GCPs from a Google Earth mosaic of 30 Quickbird images. Most of the GCPs were located on road intersections and corners of large buildings. Initially, we located 39 evenly distributed GCPs, but six of them were flagged as blunders. Closer examination of the blunders showed that they were located on six Quickbird images (four of them were taken on the same day, March 2, 2006) that had large horizontal shifts (up to 26 m) relative to the other images. 150 tie points were automatically located with AutoTie utility.

Despite the lack of calibrated camera parameters, bundle orientation reached subpixel accuracy. The RMS residuals of the 33 GCPs were X 4.53 m, Y 3.55 m, Z 5.76 m on the ground and x 0.53 pixel, y 0.64 pixel in the image space. The combination of frame camera model and strong geometry of the calibrated images resulted in a robust solution: with three GCPs, the positional accuracy degraded by only 20% (Table 2).

We generated a 60 m DEM for the Tarim testfield from frames 1 and 2 (the B/H ratio is 0.4). To estimate the DEM vertical accuracy, we used IceSAT laser altimetry data (GLA14 Global Land Surface Altimetry data, release 28) collected from 2003 to 2007 (Zwally *et al.*, 2008). The GLAS laser spots have about 65 m in diameter and 175 m separation distance. The GLAS horizontal accuracy is 10.6±4.5 m and the vertical accuracy is within ±34 cm as determined for Laser 2a on White Sands Space Harbor IceSAT verification area (Magruder *et al.*, 2007). We selected 1,203 laser points on slopes less than 3 degrees to exclude slope-related IceSAT errors. The DEM errors were estimated by subtracting IceSAT elevations from the DEM elevations at the corresponding locations (Figure 5). The RMSE for 1,203 laser points was 6.18 m with a 3.7 m bias.

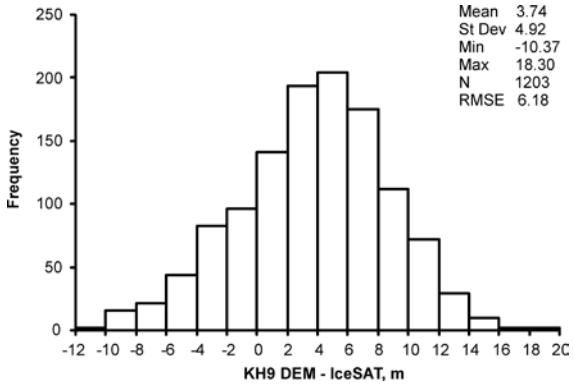

Figure 5. Frequency distribution of the differences between KH-9 DEM and IceSAT points.

Akshiirak testfield

We collected 13 GCPs in a lower area that surrounds the glacier and snow covered mountain range. Since only natural features (lake shores and rock outcrops) were used for image orientation, the positional accuracy was lower (ground RMSE X 6.55 m Y 9.80 m Z 11.41 m, image RMSE x 1.09, y 1.20).

We generated a DEM for the Akshiirak testfield from three stereopairs: frames 1-2, 2-3 and 1-3 (B/H 0.4 and 0.9) (Figure 6). The advantage of using three stereopairs is a more accurate and detailed DEM. LPS first generated separate sets of matched points per stereopair and then merged the sets before converting them to a raster. When we compared the point sets themselves (an optional ATE output), we found that they complement each other on very steep terrain slopes that are in 'blind' areas of a single stereopair. Due to the low optical contrast of the snow fields in the center of the Akshiirak range, a few areas of low DEM definition and mismatched points are visible. This suggests that the KH-9 DEM can be particularly useful to patch SRTM DEM that have good vertical accuracy over flat snow fields, but have voids on steep slopes.

To estimate vertical accuracy of the KH-9 DEM, we compared a DEM fragment (10x5 km) to a reference DEM digitized from a 1:25,000 topographic map (Figure 6, white box). The test area is located in the narrow valley of Eer-Tash river with steep (up to 76°) rock slopes and elevations from 3,101 m to 4,215 m (Figure 7). The area was selected to exclude a possible elevation bias related to the lowering of the glacier surface due to melting. The RMSE was 20.0 m with a bias of 6.9 m.

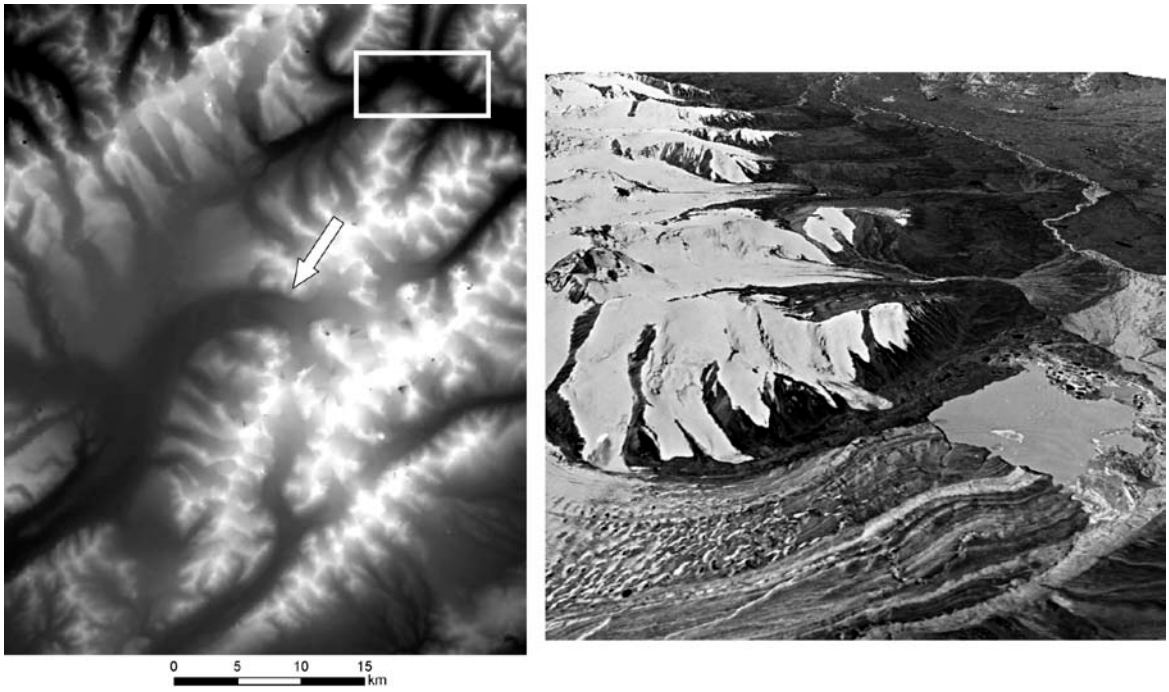

Figure 6. KH-9 DEM generated for the Akshiirak test area (left) and a perspective view in the direction of the white arrow in the left figure (right). The white box shows the area selected for accuracy estimation.

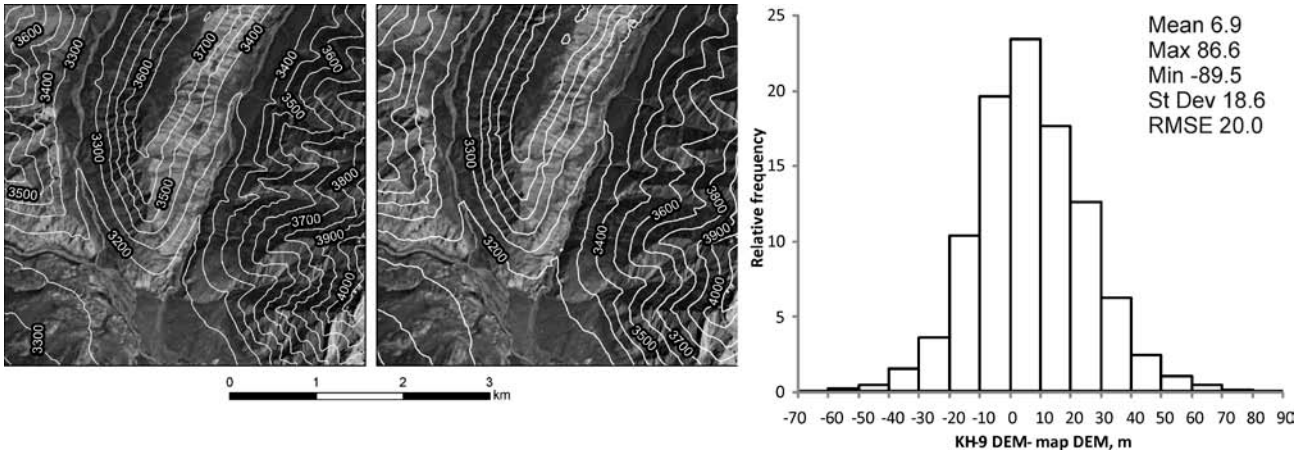

Figure 7. 100 m contour lines from 1:25,000 topographic map (left) and KH-9 DEM (center) overlaid on orthorectified KH-9 image and frequency distribution of the differences between the KH-9 and map-based DEMs

Conclusion

In this paper we demonstrated that declassified KH-9 Hexagon imagery is suitable for generation of 6 m resolution orthoimages and DEMs over large areas with minimum GCPs (in this study, for example, 120x120 km with 3 GCPs). The image distortions of the scanned KH-9 frames (9x18 in) were assessed using coordinates of reseau grid marks exposed on the film. We found non-uniform image distortions (mean 12.74 μm, max 68.88 μm) that were removed by local interpolation. In bundle orientation of KH-9 image triplets, we achieved horizontal accuracies below 6 m for a flat terrain testfield and approximately 10 m for a mountainous terrain testfield. With three GCPs the image orientation accuracy degraded by only 20%. We generated a DEM from the KH-9 images and estimated its vertical accuracy using IceSAT laser altimetry data and an additional DEM from 1:25,000 topographic maps. The DEM RMSE was 6.18 m over flat terrain and 20.0 m over mountainous terrain.

Acknowledgments

This work was supported by NASA NNH04ZYS005N grant. We thank Google for granting permission to collect GCPs. Matt Hall helped to improve the English. We also thank two anonymous reviewers for their comments on the manuscript.

References

Ali, A.E., 1993. The Large Format Camera in Retrospect. *Journal of King Saud University. Engineering Sciences*, 5(1):77-90.

Baclawski, J.A., 1997. Corona: the foundation for a mapmaking revolution. *Corona: between the Sun and the Earth. The first NRO reconnaissance eye in space*, (R. A. McDonald, editor), American Society for Photogrammetry and Remote Sensing, Bethesda, MD, pp. 231-241.

Baltsavias, E.P., 1999. On the Performance of Photogrammetric Scanners. *Photogrammetric Week*:155-173.

Day, D.A., J.M. Longson, and B. Latell (editors), 1998. *Eye in the Sky: The Story of the Corona Spy Satellites*, Smithsonian Institution Press, Washington, D.C., 303 p.

Derenyi, E., and L. Newton, 1986. Accuracy of three dimensional coordinate determination using Large Format Camera photography. *International Archives of Photogrammetry and Remote Sensing*, 26(4):14-22.

Galiatsatos, N., 2004. *Assessment of the CORONA series of satellite imagery for landscape archaeology: A case study from the Orontes valley, Syria*. Ph.D. dissertation, University of Durham, Durham, 373 p.

Magruder, L.A., C.E. Webb, T.J. Urban, E.C. Silverberg, and B.E. Schutz, 2007. ICESat Altimetry Data Product Verification at White Sands Space Harbor. *IEEE Transactions on Geoscience and Remote Sensing*, 45(1):147-155.

McDonald, R.A. (editor), 1995. *CORONA Between the Sun and the Earth The First NRO Reconnaissance Eye in Space*, American Society for Photogrammetry and Remote Sensing, Bethesda, Maryland, 440 p.

Mollberg, B.H., and B.B. Schardt, 1988. *Mission report on the Orbiter Camera Payload System (OCPS) Large Format Camera (LFC) and Attitude Reference System (ARS)*, NASA, Houston, Texas, 341 p.

National Archives and Records Administration, 2002. *Press Release. National Archives Releases Recently Declassified Satellite Imagery*. URL: http://www.archives.gov/press/press-releases/2003/nr03-02.html , (last date accessed: 16 March 2009).

Newton, L., and E. Derenyi, 1986. Control extension utilizing large frame camera imagery. *Proceedings of the 52nd Annual meeting of the American Society of Photogrammetry and Remote Sensing*, (American Society for Photogrammetry and Remote Sensing, Washington, D.C.), pp. 456-465.

NGA, 2002. Historical imagery declassification, URL: http://www.nga.mil/portal/site/nga01/index.jsp?epi-content=GENERIC&itemID=5b08f8d62404af00VgnVCMServer23727a95RCRD&beanID=1629630080&viewID=FAQ, (last date accessed: 16 March 2009).

Peebles, C., 1997. *The Corona project : America's first spy satellites*, Naval Institute Press, Annapolis, Maryland, 351 p.

Richelson, J.T., 2001. *The wizards of Langley: inside the Cia's directorate of science and technology*, Westview Press, Boulder, Colorado, 416 p.

Togliati, G., and R. Moriondo, 1986. Large Format Camera: the second generation photogrammetry camera for space cartography. *Internal Report*, Politechnico di Milano, Milan, Italy.

Zwally, H.J., R. Schutz, C. Bentley, J. Bufton, T. Herring, J. Minster, J. Spinhime, and R. Thomas, 2008. *GLAS/ICESat L2 Global Land Surface Altimetry Data, Release 28*, National Snow and Ice Data Center, Boulder, Colorado.